arXiv:1603.01054v1 [physics.optics] 3 Mar 2016

Dynamics of Localized Structures in Systems with Broken Parity Symmetry

J. Javaloyes,[1] P. Camelin,[2] M. Marconi,[2] and M. Giudici[2]

[1] *Departament de Física, Universitat de les Illes Baleares, C/Valldemossa km 7.5, 07122 Mallorca, Spain*
[2] *Institut Non-Linéaire de Nice, Université de Nice Sophia Antipolis, CNRS UMR 7335, 06560 Valbonne, France*

A great variety of nonlinear dissipative systems are known to host structures having a correlation range much shorter than the size of the system. The dynamics of these Localized Structures (LSs) have been investigated so far in situations featuring parity symmetry. In this letter we extend this analysis to systems lacking of this property. We show that the LS drifting speed in a parameter varying landscape is not simply proportional to the parameter gradient, as found in parity preserving situations. The symmetry breaking implies a new contribution to the velocity field which is a function of the parameter value, thus leading to a new paradigm for LSs manipulation. We illustrate this general concept by studying the trajectories of the LSs found in a passively mode-locked laser operated in the localization regime. Moreover, the lack of parity affects significantly LSs interactions which are governed by asymmetrical repulsive forces.

PACS numbers: 42.65.Sf, 42.65.Tg, 47.20.Ky, 89.75.Kd

Symmetry breaking (SB) is undoubtedly one of the most important phenomenon occurring in nature [1–3]. One distinguishes the situations of spontaneous SB, where the governing laws are symmetrical but some of the solutions are not, from the cases of explicit SB where the symmetry of the underlying theory is broken. In Optics, spontaneous SB has been identified in pattern formation [4], coupled nanocavities [5], ring lasers [6] and two dimensional [7] or vectorial [8] solitons. Explicit SB is known to induce convective instabilities [9–13] and drifts [14–16] and was recently studied in PT symmetric waveguides [17, 18].

We address here dissipative extended systems hosting Localized Structures (LSs) which are solutions characterized by a correlation length much smaller than the size of the system making them individually addressable [19–21]. These states are ubiquitous [22–28] but they are particularly relevant for applications when implemented in optical resonators and used as light bits for information processing [28–31]. Localized structures were observed in the transverse [32] and longitudinal [33, 34] dimensions of optical resonators driven by an external field, in lasing cavities [35, 36] and in optical parametric oscillators [37, 38]. Several theoretical paradigms have been used to describe these situations, including the Lugiato-Lefever [39] and the Rosanov or Ginzburg-Landau equations [40]. All these systems share invariance under the mirror symmetry of the variables in which localization occurs. When LSs are implemented in the transverse section of semiconductor microcavities, an additional equation accounts for carriers dynamics but it still preserves the overall parity [32] and the hosted LSs are motionless when the underlying medium is homogeneous. Because of translational invariance, LSs exhibit a Goldstone mode [30, 41] which is excited by any inhomogeneous parameter variation, inducing their motion [42–44]. Since the velocity, instead of the acceleration, is proportional to the parameter variations, the latter is interpreted as an Aristotelian force.

More recently, delayed systems have been analyzed from the perspective of their equivalence with spatial extended systems [45] and proposed for hosting LSs, fronts and chimera states [46–50]. In general, the non-instantaneous and causal response of the medium implies a lack of parity in their spatiotemporal representation. In this letter we show that, in an explicitly parity broken system, the dynamics of temporal LSs in a modulated parameter landscape is fundamentally different from the ones found in parity preserving situations. While in the latter the motion of the LSs depends exclusively on the parameter gradient, we reveal the existence in the former of another contribution inducing a dependence of the velocity field on the local parameter value. We consider an experimental situation where this contribution is dominant and we formulate a new paradigm for LSs manipulation. Moreover, we show that parity breaking leads to asymmetrical repelling forces between LSs.

In a parity broken system, traveling waves are the only possible solutions and the behavior of LSs can be described considering a generic partial differential equation (PDE) for a field $E(z,t)$

$$\frac{\partial E}{\partial t} + \upsilon(\mu)\frac{\partial E}{\partial z} = \mu E + \mathcal{F}\left(|E|^2, \frac{\partial^2}{\partial z^2}\right)E + Y. \quad (1)$$

with $\mathcal{F}$ a general nonlinear function whose explicit expression is not needed. We note that equation (1) encompasses the cases previously mentioned [39, 40] and we assume that it supports drifting LSs solutions defined as $E(z,t) = p(z - \upsilon t)$ with $p(u)$ an even function. For the sake of clarity, Eq.(1) is written in a comoving frame such that $\upsilon(\mu_0) = 0$. Experimentally, when a single parameter is modulated, it may affect several terms of the PDE and we consider the most general case where the modulation affects an even and an odd derivative, i.e. the linear gain μ and the drift velocity $\upsilon(\mu)$. The influence of a small parameter variation $\mu = \mu_0 + m(z)$ can be studied by a variational approach [51] writing $E = p[z - z_0(t)]$ which allows finding that the position z_0 of the LS evolves according to

$$\frac{dz_0}{dt} = \left\{\frac{\int p^\dagger \cdot pz dz}{-\int p^\dagger \cdot \dot{p} dz}\right\}\frac{dm}{dz}(z_0) + \left\{\frac{d\upsilon}{d\mu}(\mu_0)\right\}m(z_0) \quad (2)$$

with $a\cdot b$ the dot product of complex numbers, and $p^\dagger$ and $\dot{p}$ two odd eigenfunctions representing the adjoint and direct neutral translation modes. Because of the term $(dv/d\mu)$ coming from SB, the LS speed is proportional to the local value of the parameter $m(z)$; if this term is neglected, one recovers the case where LS motion is purely proportional to the gradient of $m(z)$.

These general considerations can be applied to the case of LSs hosted in a laser field $E(z,t)$ coupled to a distant Saturable Absorber (SA). While this scheme leads to conventional passive mode-locking (PML) for cavity roundtrips τ shorter than the gain recovery time $\tau < \tau_g$, we operate in the long cavity regime $\tau \gg \tau_g$, and for bias currents below the lasing threshold of the compound system. In this regime the PML pulses become *localized*, i.e they become lasing LSs [52] which can be individually addressed by an optical/electrical perturbation [53]. By denoting $G(z,t)$ the gain and $Q(z,t)$ the saturable absorption, the Haus equations [54] governing their dynamics reads

$$\frac{\partial E}{\partial t} = \left[\sqrt{\kappa}\left(1+\frac{1-i\alpha}{2}G-\frac{1-i\beta}{2}Q\right)-1+d\frac{\partial^2}{\partial z^2}\right]E, \quad (3)$$

$$\frac{\partial G}{\partial z} = \Gamma G_0 - G\left(\Gamma+|E|^2\right), \frac{\partial Q}{\partial z} = Q_0 - Q\left(1+s|E|^2\right) \quad (4)$$

where time has been normalized to the SA recovery time, α and β are the linewidth enhancement factor of the gain and absorber sections, κ the fraction of the power remaining in the cavity after each roundtrip, G_0 the pumping rate, $\Gamma = \tau_g^{-1}$ the gain recovery rate, Q_0 the modulation depth of the SA, s the ratio of the saturation energy of the SA and of the gain sections and $d = \left(2\gamma^2\right)^{-1}$ with γ the bandwidth of the spectral filter. In Eq.(3), the spatial variable z denotes the propagation along the cavity axis and corresponds to a fast temporal scale for the LSs evolution within the cavity roundtrip while t is the slowly evolving time scale related to the LSs evolution after each roundtrip. The steady states of Eqs.(3,4) are the periodic solutions of the PML laser and Eqs.(3,4) are subject to periodic boundary conditions $(E,G,Q)(z+\tau,t) = (E,G,Q)(z,t)$.

As the Eqs.(4) are only first order in z, LSs stem here from a parity broken PDE and they exhibit a strong drift. The adiabatic elimination of G and Q would cancel such a drift and reduce Eq.(3) to the Ginzburg-Landau Equation. Although in a semiconductor medium the adiabatic elimination of the absorption may be sound, it cannot be applied to the gain because τ_g is much longer than the pulsewidth $\tau_p \sim \gamma^{-1}$. In our case, the bias current G_0 controls at the same time the linear gain, whose expression is $\mu = \sqrt{\kappa}(2+G_0-Q_0)/2-1$, but also higher order spatial derivatives due to the non-instantaneous response of the medium. Assuming that $E \ll 1$ and $\partial_z G_0 \ll \Gamma G_0$, $G(z)$ than can be expressed as

$$G(z) \sim G_0(z)\left[1-\int_0^\infty |E(z-r)|^2 e^{-\Gamma r} dr\right]. \quad (5)$$

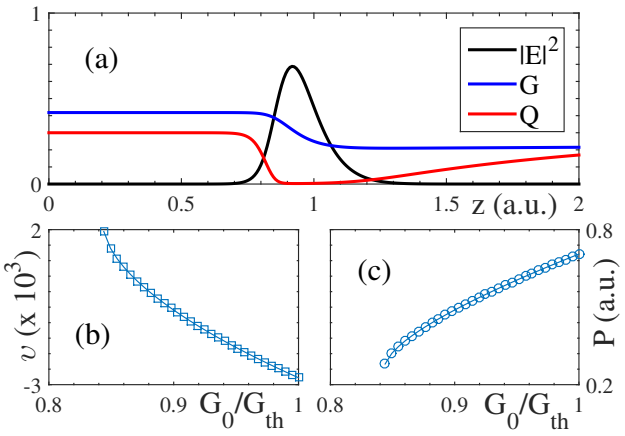


Figure 1. (a) Profiles of the field intensity $|E|^2$, the carrier G and absorption Q. (b,c) Bifurcation diagram of the stable solution branch for the drift velocity and the energy. Parameters are $(\gamma,\kappa,\alpha,\beta,\Gamma,Q_0,s) = (40,0.8,1,0.5,0.04,0.3,30)$.

Expanding $E(z-r)$ in Taylor series in r and integrating over r leads to an infinite series of even and odd derivatives of E with respect to z. The odd terms contribute to the drift of the solutions and to SB. This establishes the conceptual link with the generic situation depicted in Eq.1.

The Eqs.(3-4) were solved in [52] for the LSs energy; here we calculate also the LS drift velocity as a function of the bias current. A typical asymmetrical profile can be observed in Fig.1(a) while the bifurcation diagrams are depicted in Fig.1(b,c). The solution branch for the energy of the pulse $P = \int_{-\infty}^{\infty}|E|^2 dz$ depicted in Fig.1(c) shows the typical square root behavior consistent with the fact that the LSs arise as a saddle-node bifurcation of limit cycle [52]. Importantly, one notices that the drift velocity, or equivalently the deviation of the period with respect to the roundtrip, is a strongly evolving function of the bias current. The lack of the $(z \to -z)$ symmetry is ultimately a consequence of the causality principle, because the response of the medium is necessarily asymmetric with respect to an intensity variation, as shown in Fig.1(a) and Eq.5.

Experimental evidence of this phenomenon is obtained using the setup described in [52, 53] and by modulating the pumping current of a VCSEL mounted in an external cavity closed by a resonant saturable absorber mirror. When the modulation frequency ν_m is almost resonant with the cavity free spectral range ν_c, i.e. small values of the detuning $\Delta = \nu_m - \nu_c$, a quasi-stationary parameter variation is introduced inside the cavity. In line with the theoretical analysis, LSs' dynamics in this parameter landscape can be pictured using a pseudo spatio-temporal representation, where the temporal trace is folded onto itself after a time that corresponds to the cavity roundtrip ν_c^{-1}. Accordingly, the roundtrip number n becomes a slow time variable proportional to t while

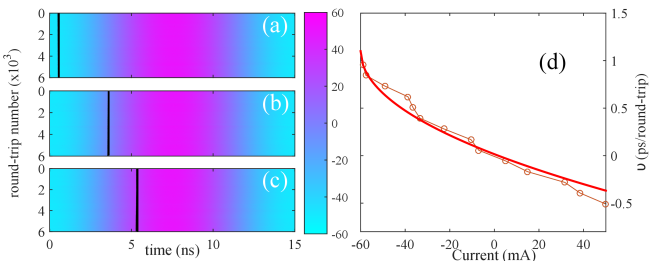


Figure 2. a-c) Spatio-temporal diagrams of the LS position evolution (black line) when the current is sinusoidally modulated (color scale in mA) with an amplitude $\delta J = 120\,\mathrm{mA}$ around $J_{cw} = 226\,\mathrm{mA}$ and $\nu_m = 66614250\,\mathrm{Hz}$. The detunings are : a) $\Delta = -4.75\,\mathrm{KHz}$, b) $\Delta = -0.25\,\mathrm{kHz}$ and c) $\Delta = 1.75\,\mathrm{kHz}$. d) LS drifting speed induced by the variation of J (circle) and best fit with a square-root function.

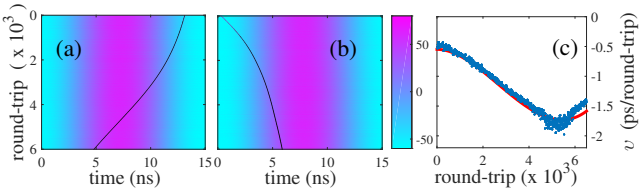


Figure 3. (a,b) Spatiotemporal diagrams of the LS position evolution (black line) over the current modulation (color scale in mA). (a)$\Delta = -9.25\,\mathrm{kHz}$, (b) $\Delta = 3.25\,\mathrm{KHz}$, all other parameters as in Fig. 2. (c) LS drifting speed (red) calculated from the derivative of the trajectory shown in (a) and calculated as $\upsilon_\Delta + \upsilon_J$ (dots) with υ_J obtained fitting the curve υ_J in Fig. 2d) with J the value of the current along the trajectory.

the pseudo-space variable z corresponds to the position within the roundtrip [45]. However, to simplify the interpretation, we present these diagrams in the reference frame of the modulation signal, i.e. using a folding parameter ν_m^{-1}.

We first modulate sinusoidally the pumping current around $J = J_{cw}$ and we represent in Fig.2(a-c) the evolution of LS position on the current modulation landscape. When $\Delta = 0$ the LS exhibits a fixed position with respect to the modulation signal which is located on the zero of the modulation on its positive slope. If $|\Delta|$ is small enough ($-4.75\,\mathrm{kHz} < \Delta < 2.5\,\mathrm{kHz}$), the LS still sits in a stationary position with respect the modulation signal. We shows in Fig.2(a,c) that this position gets closer to the modulation peak (resp. bottom) for increasing positive (resp. negative) value of Δ. It is worth noting that all stationary positions found varying Δ are located on the positive slope of the modulation. The presence of a finite Δ should induce a drifting speed υ_Δ which is given by $\upsilon_\Delta = \Delta\nu_c^{-2}$ in the limit of $\Delta \ll \nu_c$. The fact that the LS remains locked to stationary positions in the modulation, as shown in Fig.2(a,c), indicates that another Aristotelian force equilibrates υ_Δ.

These results can be explained by assuming that a current variation around $J = J_{cw}$ induces a drifting speed υ_J of the LS which depends on the value of J instead of its time derivative, as suggested by the theoretical analysis. At each stationary position found for a given $\Delta \neq 0$, υ_Δ is compensated by an opposite drifting speed induced by current variation υ_J such that $\upsilon_\Delta + \upsilon_J = 0$. Accordingly, from the value of the current at the stationary positions, it is possible to establish the dependence of υ_J on $(J - J_{cw})$, as shown in Fig.2(d). In agreement with the theory, υ_J is a decreasing function of J. This explains why the stable equilibrium points are located only on the positive slope of the modulation: J plays a restoring (diverging) role on positive (negative) slope with respect to deviations from the equilibrium point.

For values of Δ outside the above specified interval, υ_Δ cannot be balanced by υ_J at any current values spanned by the modulation and the LS starts to drift in the space-time diagram, as shown in Fig.3(a,b), in a way reminiscent of the Adler unlocking mechanism of a forced oscillator. In the limit of large detuning, the motion becomes uniform because $|\upsilon_\Delta| \gg |\upsilon_J|$. From the LS time law, extracted from Fig.3(a), we infer the instantaneous velocity of the LS in the space-time diagram, that we represent in Fig.3(c), red curve. On the other hand, the speed can also be calculated by adding $\upsilon_\Delta + \upsilon_J$, where the first addendum is obtained from the value of Δ and the second is obtained from the curve $\upsilon_J(J - J_{cw})$ plotted in Fig.2(d), using the value of J corresponding to the position of the LS on the modulation landscape. The results obtained are represented in Fig.3(c) using blue dots. The two curves representing the instantaneous velocity coincide, thus indicating that LS's speed depends only on the local current value, while the derivative of the modulation signal is not playing any relevant role.

We realized another experiment using a bivalued rectangular current modulation with upper and lower values $J_{u,l}$. Because a large set of current values is spanned at the pulse rising edge, it becomes an anchoring region for the LSs for a wide set of values of Δ. Yet, when Δ falls outside the locking interval, the LS drifts in the space-time diagram and it exhibits two clearly different speeds in the regions where $J = J_u$ and $J = J_l$. This gives further evidence that LS speed does not depend on the time derivative of the modulation, otherwise it would be identical on the two current plateaus.

When several LSs are present into the cavity, interaction forces come into play and the current landscape enables their analysis. The LSs evolution when the rectangular current modulation is suddenly applied at roundtrip $N = 800$ is shown in Fig.4(a). Let us identify the LSs from 1 to 3 using their position from left to right. The LS_3 acquires a strong negative speed when passing on the high current plateau as $J_u > J_{cw}$ while the two leftmost LSs acquire a positive speed since $J_l < J_{cw}$. All the LSs try to reach the rising edge of the modulation but, when LS_2 and LS_3 get too close at $N = 4500$, repulsive interaction prevents LS_3 to occupy the stable equilibrium position where $\upsilon_\Delta + \upsilon_J = 0$, which is instead occupied

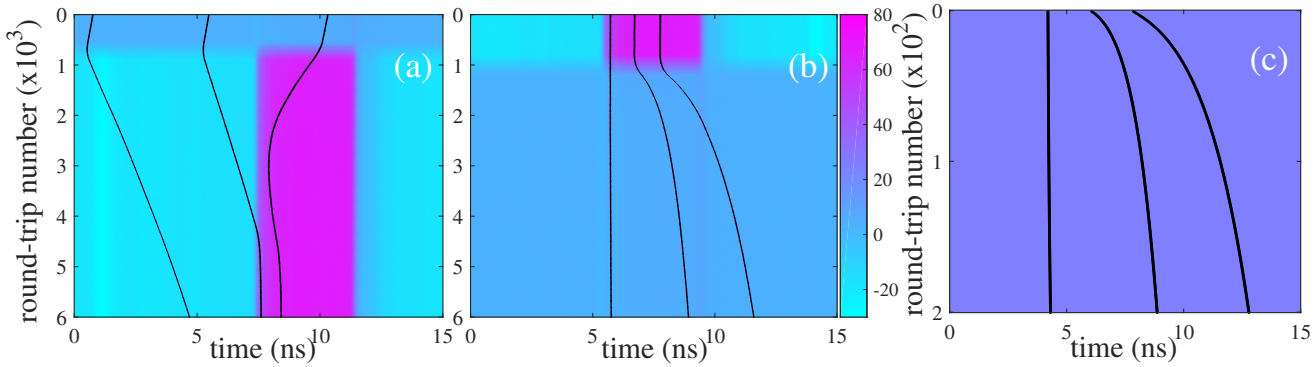


Figure 4. Experimental spatiotemporal diagrams showing the evolution of three LSs when an electrical square pulse of 4 ns is applied (a) and removed (b) to the pumping current (color scale in mA). The current pulse amplitude is 120 mA and $J_{cw} = 220$ mA. In (b) $\Delta = 0$, while Δ is slightly negative in (a) explaining the negative drifting speed from $N = 0$ until $N = 800$. Panel c): Numerically calculated trajectory using Eqs. (8,9), with parameters $(v_0, \Delta v, P_0, \Delta P) = (0, -0.01, 0.28, 0.7)$, $G_{sn} = 0.845 G_{th}$ and $v_\Delta = -2.35 \times 10^{-3}$. Other parameters as in Fig.1.

by LS_2. Hence, LS_3 sits at a position shifted of 0.8 ns, where the repulsive force generated by LS_2 force balances the Aristotelian forces $v_\Delta + v_J(J_u - J_{cw})$. This situation further evolves (not shown in Fig.4(a)) when LS_1 reaches the rising front and pushes the other two LSs to the right to occupy the position previously occupied by LS_2. The three LSs then remain eventually gathered around the rising front of the electrical pulse at a mutual distance of 0.8 ns. This situation is similar to the one shown in Fig.4(b) before the modulation is removed at $N = 1200$. Hereafter, the LSs evolve exclusively under the action of repulsive forces and their dynamics reveal that the action-reaction principle is violated as for instance LS_1 interacts with LS_2 but not vice-versa. The asymmetry of the interaction is due to the broken parity and follows from the causality principle.

Such a dynamics in a modulated parameter landscape can be theoretically analyzed with the results of Fig.1. Close to the saddle-node bifurcation, we approximate the drift as a function of the current as

$$v = f_v(G_0) = v_0 + \Delta v \sqrt{G_0 - G_{sn}}, \tag{6}$$

and similarly $P = f_P(G_0)$. The coefficients $(v_0, \Delta v, P_0, \Delta P)$ and G_{sn} are given by the bifurcation diagram of a single LS in Fig.1(b,c). In the comoving frame of the external periodic potential, the equation for the relative drift velocity Eq.(6) transforms into $\tilde{v} + v_\Delta = f_v(G_0)$ with v_Δ the velocity of the drifting potential and $\tilde{v}$ the residual speed. In this reference frame, the external potential depends only on the fast time z and not anymore on the slow time t. As the characteristics of the PML pulses depend only on the gain value at the leading edge $G^{(i)}$, we replace in Eq.(6) $G_0 \to G^{(i)}$. During the gain depletion occurring around the pulse, the so-called fast stage, only the strongly nonlinear stimulated terms in Eqs.(4) are relevant and the gain at the falling edge of the LS is simply $G^{(f)} = G^{(i)} \exp(-P)$. Provided that the variations of the bias current $G_0(z)$ are slower than τ_g, the solution of the carrier equation in between LSs reads

$$G(z_2) = G(z_1) e^{-\Gamma D_2} + G_0(z_2)\left(1 - e^{-\Gamma D_2}\right), \tag{7}$$

with $D_n = z_n - z_{n-1}$ and $G(z_1)$ an arbitrary initial condition. By denoting as z_n the position of the n-th LS whose residual velocity is $\tilde{v}_n = dz_n/dt$ we find that

$$\frac{dz_n}{dt} = f_v\left[G_n^{(i)}\right] - v_\Delta\ ,\ P_n = f_P\left[G_n^{(i)}\right], \tag{8}$$

$$G_n^{(i)} = G_{n-1}^{(i)} e^{-P_{n-1} - \Gamma D_n} + G_0(z)\left(1 - e^{-\Gamma D_n}\right). \tag{9}$$

For $N-$LSs with $n \in [1, \ldots, N]$, the periodic boundary conditions linking the gain depletion of the rightmost LS to the dynamics of the leftmost is $z_0 = z_N - \tau$. The repulsive interactions mediated by the gain depletion is exemplified in Fig.4c), where, as shown in the experiment, LS_n affects LS_{n+1} but not vice-versa. The source of the asymmetry is visible in Eq.(9) and the interactions are repulsive since the velocity is a decreasing function of the current ($\Delta v < 0$).

In conclusion, we described the dynamics of LSs in systems with an explicitly broken parity symmetry appearing because of the causality principle. Our analysis reveals that the Aristotelian forces ruling their dynamical behavior are very different from the ones found in parity preserving conditions. These results pave the way towards control and manipulation of LSs for information processing in broken parity systems and in particular to the control of three dimensional light bullets in semiconductor lasers [55].

ACKNOWLEDGMENTS

J.J. acknowledges financial support from the Ramón y Cajal fellowship and project COMBINA (TEC2015-65212-C3-3-P). The INLN Group acknowledges funding

of Région PACA with the Projet Volet Général 2011 GEDEPULSE and ANR project OPTIROC.

[1] F. Englert and R. Brout. Broken symmetry and the mass of gauge vector mesons. *Phys. Rev. Lett.*, 13:321–323, Aug 1964.

[2] Patrick P.L Tam and Richard R Behringer. Mouse gastrulation: the formation of a mammalian body plan. *Mechanisms of Development*, 68(1-2):3 – 25, 1997.

[3] Julyan H. E. Cartwright, Juan Manuel García-Ruiz, Oreste Piro, C. Ignacio Sainz-Díaz, and Idan Tuval. Chiral symmetry breaking during crystallization: An advection-mediated nonlinear autocatalytic process. *Phys. Rev. Lett.*, 93:035502, Jul 2004.

[4] C. Green, G. B. Mindlin, E. J. D'Angelo, H. G. Solari, and J. R. Tredicce. Spontaneous symmetry breaking in a laser: The experimental side. *Phys. Rev. Lett.*, 65:3124–3127, Dec 1990.

[5] P. Hamel, S. Haddadi, F. Raineri, P. Monnier, G. Beaudoin, I. Sagnes, A. Levenson, and A. M. Yacomotti. Spontaneous mirror-symmetry breaking in coupled photonic-crystal nanolasers. *Nat Photon*, 9(5):311–315, May 2015. Letter.

[6] S. Beri, L. Gelens, M. Mestre, G. Van der Sande, G. Verschaffelt, A. Scire, G. Mezosi, M. Sorel, and J. Danckaert. Topological insight into the non-arrhenius mode hopping of semiconductor ring lasers. *Physical Review Letters*, 101(9):093903, 2008.

[7] V. Skarka, N. B. Aleksić, M. Lekić, B. N. Aleksić, B. A. Malomed, D. Mihalache, and H. Leblond. Formation of complex two-dimensional dissipative solitons via spontaneous symmetry breaking. *Phys. Rev. A*, 90:023845, Aug 2014.

[8] C. Cambournac, T. Sylvestre, H. Maillotte, B. Vanderlinden, P. Kockaert, Ph. Emplit, and M. Haelterman. Symmetry-breaking instability of multimode vector solitons. *Phys. Rev. Lett.*, 89:083901, Jul 2002.

[9] A. Couairon and J. M. Chomaz. Pattern selection in the presence of a cross flow. *Phys. Rev. Lett.*, 79:2666–2669, Oct 1997.

[10] Marco Santagiustina, Pere Colet, Maxi San Miguel, and Daniel Walgraef. Noise-sustained convective structures in nonlinear optics. *Phys. Rev. Lett.*, 79:3633–3636, Nov 1997.

[11] Namiko Mitarai and Hiizu Nakanishi. Spatiotemporal structure of traffic flow in a system with an open boundary. *Phys. Rev. Lett.*, 85:1766–1769, Aug 2000.

[12] H. Ward, M. N. Ouarzazi, M. Taki, and P. Glorieux. Influence of walkoff on pattern formation in nondegenerate optical parametric oscillators. *Phys. Rev. E*, 63:016604, Dec 2000.

[13] A. Mussot, E. Louvergneaux, N. Akhmediev, F. Reynaud, L. Delage, and M. Taki. Optical fiber systems are convectively unstable. *Phys. Rev. Lett.*, 101:113904, Sep 2008.

[14] M. Tlidi, L. Bahloul, L. Cherbi, A. Hariz, and S. Coulibaly. Drift of dark cavity solitons in a photonic-crystal fiber resonator. *Phys. Rev. A*, 88:035802, Sep 2013.

[15] François Leo, Arnaud Mussot, Pascal Kockaert, Philippe Emplit, Marc Haelterman, and Majid Taki. Nonlinear symmetry breaking induced by third-order dispersion in optical fiber cavities. *Phys. Rev. Lett.*, 110:104103, Mar 2013.

[16] Pedro Parra-Rivas, Damià Gomila, François Leo, Stéphane Coen, and Lendert Gelens. Third-order chromatic dispersion stabilizes kerr frequency combs. *Opt. Lett.*, 39(10):2971–2974, May 2014.

[17] I. V. Barashenkov, Sergey V. Suchkov, Andrey A. Sukhorukov, Sergey V. Dmitriev, and Yuri S. Kivshar. Breathers in $\mathcal{PT}$-symmetric optical couplers. *Phys. Rev. A*, 86:053809, Nov 2012.

[18] N. V. Alexeeva, I. V. Barashenkov, Andrey A. Sukhorukov, and Yuri S. Kivshar. Optical solitons in $\mathcal{PT}$-symmetric nonlinear couplers with gain and loss. *Phys. Rev. A*, 85:063837, Jun 2012.

[19] M. Tlidi, P. Mandel, and R. Lefever. Localized structures and localized patterns in optical bistability. *Phys. Rev. Lett.*, 73:640–643, Aug 1994.

[20] P. Coullet, C. Riera, and C. Tresser. Stable static localized structures in one dimension. *Phys. Rev. Lett.*, 84:3069–3072, Apr 2000.

[21] O. Descalzi, M. Clerc, S. Residori, and G. Assanto. *Localized States in Physics: Solitons and Patterns*, volume 751 of *Lecture Notes in Physics*. Springer Berlin Heidelberg, 2011.

[22] J. Wu, R. Keolian, and I. Rudnick. Observation of a nonpropagating hydrodynamic soliton. *Phys. Rev. Lett.*, 52:1421–1424, Apr 1984.

[23] E. Moses, J. Fineberg, and V. Steinberg. Multistability and confined traveling-wave patterns in a convecting binary mixture. *Phys. Rev. A*, 35:2757–2760, Mar 1987.

[24] F. J. Niedernostheide, M. Arps, R. Dohmen, H. Willebrand, and H. G. Purwins. Spatial and spatio-temporal patterns in pnpn semiconductor devices. *physica status solidi (b)*, 172(1):249–266, 1992.

[25] Kyoung-Jin Lee, William D. McCormick, John Pearson, and Harry L. Swinney. Experimental observation of self-replicating spots in a reaction-diffusion system. *Nature*, 369:215–218, 1994.

[26] P. B. Umbanhowar, F. Melo, and H. L. Swinney. Localized excitations in a vertically vibrated granular layer. *Nature*, (382):793–796, 1996.

[27] Yuri A. Astrov and H.G. Purwins. Plasma spots in a gas discharge system: birth, scattering and formation of molecules. *Physics Letters A*, 283(5-6):349 – 354, 2001.

[28] L.A. Lugiato. Introduction to the feature section on cavity solitons: An overview. *Quantum Electronics, IEEE Journal of*, 39(2):193–196, 2003.

[29] N. N. Rosanov and G. V. Khodova. Autosolitons in bistable interferometers. *Opt. Spectrosc.*, 65:449, 1988.

[30] W. J. Firth and A. J. Scroggie. Optical bullet holes: Robust controllable localized states of a nonlinear cavity. *Phys. Rev. Lett.*, 76:1623–1626, Mar 1996.

[31] M. Brambilla, L. A. Lugiato, F. Prati, L. Spinelli, and W. J. Firth. Spatial soliton pixels in semiconductor devices. *Phys. Rev. Lett.*, 79:2042–2045, 1997.

[32] S. Barland, J. R. Tredicce, M. Brambilla, L. A. Lugiato, S. Balle, M. Giudici, T. Maggipinto, L. Spinelli, G. Tis-

soni, T. Knödl, M. Miller, and R. Jäger. Cavity solitons as pixels in semiconductor microcavities. *Nature*, 419(6908):699–702, Oct 2002.

[33] F. Leo, S. Coen, P. Kockaert, S.P. Gorza, P. Emplit, and M. Haelterman. Temporal cavity solitons in one-dimensional kerr media as bits in an all-optical buffer. *Nat Photon*, 4(7):471–476, Jul 2010.

[34] T. Herr, V. Brasch, J. D. Jost, C. Y. Wang, N. M. Kondratiev, M. L. Gorodetsky, and T. J. Kippenberg. Temporal solitons in optical microresonators. *Nature Photonics*, 8(2):145–152, 2014.

[35] P. Genevet, S. Barland, M. Giudici, and J. R. Tredicce. Cavity soliton laser based on mutually coupled semiconductor microresonators. *Phys. Rev. Lett.*, 101:123905, Sep 2008.

[36] Y. Tanguy, T. Ackemann, W. J. Firth, and R. Jäger. Realization of a semiconductor-based cavity soliton laser. *Phys. Rev. Lett.*, 100:013907, Jan 2008.

[37] I. V. Barashenkov, S. R. Woodford, and E. V. Zemlyanaya. Interactions of parametrically driven dark solitons. i. néel-néel and bloch-bloch interactions. *Phys. Rev. E*, 75:026604, Feb 2007.

[38] I. V. Barashenkov, E. V. Zemlyanaya, and T. C. van Heerden. Time-periodic solitons in a damped-driven nonlinear schrödinger equation. *Phys. Rev. E*, 83:056609, May 2011.

[39] L. A. Lugiato and R. Lefever. Spatial dissipative structures in passive optical systems. *Phys. Rev. Lett.*, 58:2209–2211, May 1987.

[40] A. G. Vladimirov, S. V. Fedorov, N. A. Kaliteevskii, G. V. Khodova, and N. N. Rosanov. Numerical investigation of laser localized structures. *Journal of Optics B: Quantum and Semiclassical Optics*, 1(1):101, 1999.

[41] J. M. McSloy, W. J. Firth, G. K. Harkness, and G.-L. Oppo. Computationally determined existence and stability of transverse structures. ii. multipeaked cavity solitons. *Phys. Rev. E*, 66:046606, Oct 2002.

[42] F. Pedaci, P. Genevet, S. Barland, M. Giudici, and J. R. Tredicce. Positioning cavity solitons with a phase mask. *Applied Physics Letters*, 89(22):221111, 2006.

[43] F. Pedaci, S. Barland, E. Caboche, P. Genevet, M. Giudici, J. R. Tredicce, T. Ackemann, A. J. Scroggie, W. J. Firth, G.-L. Oppo, G. Tissoni, and R. Jäger. All-optical delay line using semiconductor cavity solitons. *Applied Physics Letters*, 92(1):011101, 2008.

[44] Jae K. Jang, Miro Erkintalo, Stephane Coen, and Stuart G. Murdoch. Temporal tweezing of light through the trapping and manipulation of temporal cavity solitons. *Nat Commun*, 6, Jun 2015. Article.

[45] G. Giacomelli and A. Politi. Relationship between delayed and spatially extended dynamical systems. *Phys. Rev. Lett.*, 76:2686–2689, Apr 1996.

[46] Giovanni Giacomelli, Francesco Marino, Michael A. Zaks, and Serhiy Yanchuk. Nucleation in bistable dynamical systems with long delay. *Phys. Rev. E*, 88:062920, Dec 2013.

[47] Laurent Larger, Bogdan Penkovsky, and Yuri Maistrenko. Virtual chimera states for delayed-feedback systems. *Phys. Rev. Lett.*, 111:054103, Aug 2013.

[48] Francesco Marino, Giovanni Giacomelli, and Stephane Barland. Front pinning and localized states analogues in long-delayed bistable systems. *Phys. Rev. Lett.*, 112:103901, Mar 2014.

[49] M. Marconi, J. Javaloyes, S. Balle, and M. Giudici. Vectorial dissipative solitons in vertical-cavity surface-emitting lasers with delays. *Nature Photonics*, 2015.

[50] B. Garbin, J. Javaloyes, G. Tissoni, and S. Barland. Topological solitons as addressable phase bits in a driven laser. *Nat. Com.*, 6, 2015.

[51] T. Maggipinto, M. Brambilla, G. K. Harkness, and W. J. Firth. Cavity solitons in semiconductor microresonators: Existence, stability, and dynamical properties. *Phys. Rev. E*, 62:8726–8739, Dec 2000.

[52] M. Marconi, J. Javaloyes, S. Balle, and M. Giudici. How lasing localized structures evolve out of passive mode locking. *Phys. Rev. Lett.*, 112:223901, Jun 2014.

[53] M. Marconi, J. Javaloyes, P. Camelin, D. Chaparro, S. Balle, and M. Giudici. Control and generation of localized pulses in passively mode-locked semiconductor lasers. *Selected Topics in Quantum Electronics, IEEE Journal of*, PP(99):1–1, 2015.

[54] H. A. Haus. Mode-locking of lasers. *IEEE J. Selected Topics Quantum Electron.*, 6:1173–1185, 2000.

[55] J. Javaloyes. Cavity light bullets in passively mode-locked semiconductor lasers. *Phys. Rev. Lett.*, 116:043901, Jan 2016.